Vol. 92 (1997) *ACTA PHYSICA POLONICA A* No. 1

Proceedings of the ICSC–F'96 Jaszowiec '96

INVESTIGATION OF CRYSTAL GROWTH OF $SrPrGaO_4$ AND $SrLaGaO_4$

R. UECKER, P. REICHE, S. GANSCHOW

Institute of Crystal Growth, 12489 Berlin, Germany

D.-C. UECKER

Institute of Applied Chemistry, Berlin, Germany

AND D. SCHULTZE

Federal Institute for Materials Research and Testing, Berlin, Germany

Single crystals of $SrPrGaO_4$ and $SrLaGaO_4$ have been grown using the Czochralski technique. Both materials melt incongruently at 1462°C and 1516°C. The non-stoichiometric crystals contain more strontium than the starting melts. Constitutional supercooling is retarded by special growth conditions and optimum melt composition. Because of their small mismatch both crystals are recommended as substrates for $YBa_2Cu_3O_{7-x}$ epitaxy.

PACS numbers: 81.10.Fq, 81.05.Je, 81.30.Dz

1. Introduction

Since several years oxide crystals of the type $ABCO_4$ (A = Ca, Sr, Ba, B = rare earth elements and yttrium, C = Al, Ga) with K_2NiF_4 structure have been investigated as substrates for $YBa_2Cu_3O_{7-x}$ (YBCO) epitaxy [1]. Because of their well matched lattice constants and lack of phase transitions they are suitable candidates for substrates for high-T_c superconductor films epitaxy. $ABCO_4$ substrate crystals were usually grown by the Czochralski method. Several members of this group can often be grown with good quality, by the conventional Czochralski method. Unfortunately, the most commonly used substrate crystal of this group, $SrLaGaO_4$, exhibits a troublesome behaviour in this growth technique. Similarly, another $ABCO_4$ crystal containing strontium and gallium, the recently reported new candidate $SrPrGaO_4$ [2], is not easily grown by the usual Czochralski procedure.

Because of the similarity of the growth problems of both crystals these might be typical within certain limits and can occur more or less deviating in other $ABCO_4$ crystals, too. Therefore, the purpose of this report on such crystal growth problems is to give the crystal grower some hints on principle steps to successful growth of complicated materials like the reported $ABCO_4$ candidates.

2. Crystal growth experiments

The crystals have been grown by the automatized Czochralski pulling method. Both the iridium crucible and the iridium afterheater were heated by radio frequency induction [3]. The growth atmosphere was flowing nitrogen. We choose pulling rates of 0.7–1.0 $\mathrm{mm{\cdot}h^{-1}}$ and a crystal rotation rate of 15 $\mathrm{min^{-1}}$.

The starting materials La_2O_3 (5N), Pr_6O_{11} (5N), Ga_2O_3 (5N) and $SrCO_3$ (4N) were dried, mixed, pressed and sintered following standard procedures.

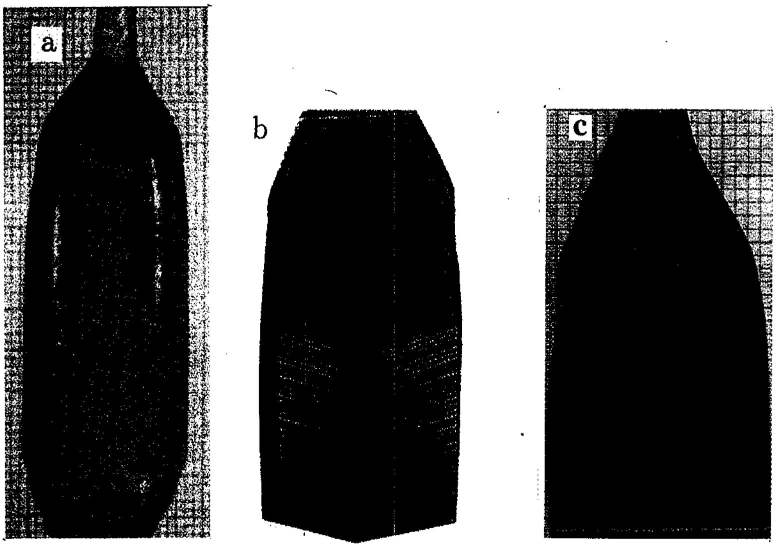

Fig. 1. (a) As-grown $SrLaGaO_4$ single crystal, (b) (100) plate of an as-grown $SrPrGaO_4$ crystal, (c) polished plate of a ⟨100⟩ grown $SrPrGaO_4$ single crystal (length 32 mm, diameter 17 mm, thickness 2 mm) after annealing in reducing atmosphere.

The growth direction was ⟨100⟩ in regard to application. The crystal growth experiments with $SrPrGaO_4$ were started with a $SrLaGaO_4$ seed crystal. We achieved crystal diameters of 18–28 mm and crystal lengths up to 75 mm. When using a melt of proper composition as described below, habits of both crystals consisted of well developed (001) planes and much less developed (101) planes. No cracks or twins have been observed. The colour of the $SrLaGaO_4$ crystals ranged between white and light yellow (see Fig. 1a). The as-grown $SrPrGaO_4$ crystals were green with red stripes parallel to the (101) facets (Fig. 1b). The red colour is attributed to higher-valent Pr^{4+} ions. Post-growth annealing in an atmosphere of 95% N_2 + 5% H_2 at about 800°C for several hours reduced Pr^{4+} to Pr^{3+}. After annealing the crystals were transparent and of green colour (Fig. 1c). Thus, optical homogeneity could be achieved in $SrLaGaO_4$ as well as in $SrPrGaO_4$ crystals.

3. Investigation of the crystallization behaviour

The stoichiometric melt compositions $SrPrGaO_4$ and $SrLaGaO_4$ did not permit the single crystal growth by the Czochralski technique. The crystalline material pulled from these melts consisted of various parts of different colour and composition and had an irregular shape [2]. Furthermore, when using molten $SrPrGaO_4$ or $SrLaGaO_4$ single crystals as new starting melt, which is a usual procedure to improve the crystal quality of congruently melting compounds by the Czochralski growth, we obtained a polyphase product. These results suggest incongruent melting of both compounds and, consequently, complex crystallization behaviour. Therefore, it was necessary to investigate the crystallization of $SrPrGaO_4$ and $SrLaGaO_4$ in the corresponding ternary systems by thermal analysis (TG-DTA).

3.1. $SrPrGaO_4$

3.1.1. Single crystals

The thermoanalytical measurements were performed using a SETARAM TG-DTA-apparatus. Samples of about 100 mg were heated and cooled at 5 K min^{-1} in Pt80/Rh 20 crucibles. First TG-DTA investigations of the crystals were carried out in air to suppress reduction and evaporation of gallium oxide. They exhibited some mass changes and complex endothermal melting effects, suggesting that redox equilibria in connection with the simultaneous appearance of Pr^{3+} and Pr^{4+} can play an important role during melting and crystallization. Subsequent DTA investigations for the explanation of the melting and, consequently, the crystallization behaviour of $SrPrGaO_4$ were carried out in an argon atmosphere.

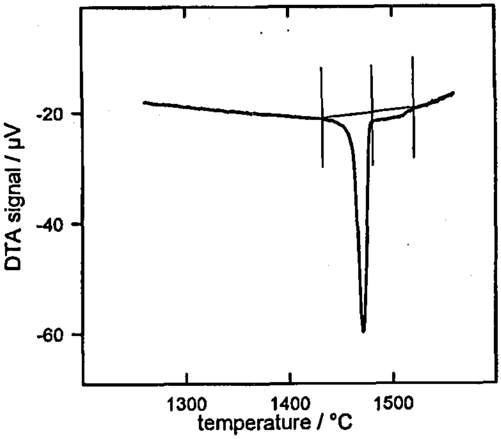

Fig. 2. DTA heating curve of grains of a $SrPrGaO_4$ single crystal.

The DTA heating curve of single crystal material shows a sharp endothermal effect starting near 1455°C associated with the melting of $SrPrGaO_4$ at 1462°C. Then a wide and very flat endothermal effect follows, ending at about 1520°C, which is caused by dissolution of a higher melting product of a peritectic decomposition (see Fig. 2). Thus, the assumed incongruent melting behaviour of $SrPrGaO_4$ was confirmed. The anticipated occurrence of the lower melting eutectic was indeed detected at about 1380°C by subsequent DTA heating and cooling curves.

3.1.2. Residual melt

The heating and cooling curves of the residual melt in air showed a distinct behaviour. Due to the considerable contents of eutectic in the residual melt, the eutectic effects (1380°C) were much stronger than before.

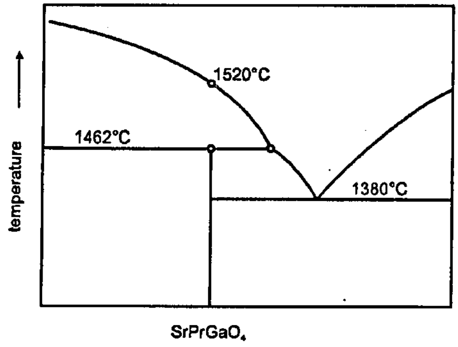

Fig. 3. Tentative phase diagram of $SrPrGaO_4$.

These DTA results led to the schematic phase diagram of the $SrPrGaO_4$ crystallization (Fig. 3). Because of the incongruent melting of $SrPrGaO_4$ the crystals cannot be grown from a melt of the same composition. A successful crystal growth is only possible if the starting melt has a concentration between the peritectic and eutectic points of the liquidus line.

3.2. $SrLaGaO_4$

3.2.1. Single crystal

The DTA heating curve in air shows a weak endothermal effect gradually starting at about 1460°C, turning to the sharp melting effect of $SrLaGaO_4$ at 1516°C. This wide melting interval suggests either a certain phase width of the $SrLaGaO_4$ phase or, more probably, the presence of impurities of eutectic. Then a wide and flat endothermal effect follows ending at about 1570°C. This latter again was caused by the dissolution of the higher melting product of a peritectic decomposition, confirming the assumed incongruent melting behaviour. The cooling process consists of a succession of crystallization effects of the higher melting phase (smaller DTA effect), the $SrLaGaO_4$ phase (larger DTA effect) and the eutectic (mp. 1465°C).

3.2.2. Sintered powders of melt composition

Before growing of the single crystals from the melt, powders of suitable composition were mixed and sintered several hours at 1200°C, followed by regrinding and another sintering treatment. By DTA of such sintered materials eutectic temperatures at about 1460°C and liquidus temperatures of about 1550°C were detected. The latter considerably exceeds the incongruent melting temperature of $SrLaGaO_4$ single crystals (1516°C). It is quite unusual that an incongruently melting compound can be grown from a melt, if its liquidus temperature is above its peritectic decomposition temperature. Here we conclude that the crystal growth does not start from the stable equilibrium. Instead, after complete melting, the melt will supercool via a metastable range until the crystallization of $SrLaGaO_4$ starts in a metastable equilibrium with the supercooled melt, probably slightly above the incongruent melting temperature. Such supercooling by *ca.* 50 K has been observed on DTA cooling curves.

Contrary to the results with $SrLaGaO_4$, we could not find any hint at such metastable crystallization of $SrPrGaO_4$.

3.2.3. Residual melt

The investigation of the residual melt by TG-DTA is under progress. A preliminary X-ray diffraction analysis proved the occurrence of a multiphase ternary eutectic besides $SrLaGaO_4$, similarly to the results of $SrPrGaO_4$ investigation.

The TG-DTA measurements of various $SrLaGaO_4$ samples allow the construction of the following schematic phase diagram of the $SrLaGaO_4$ crystallization (Fig. 4).

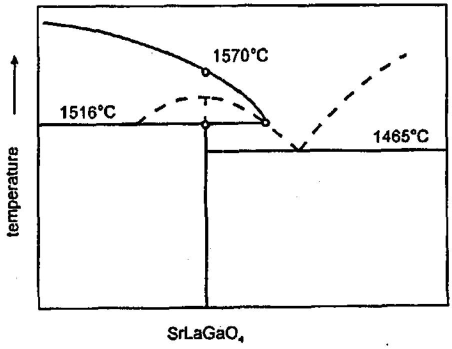

Fig. 4. Tentative phase diagram of $SrLaGaO_4$.

A similar situation as in $SrPrGaO_4$ was detected! Because of the incongruent melting behaviour of $SrLaGaO_4$ the crystals cannot be grown from a melt of their own composition, too. Usually crystal growth is possible in the concentration range of the melt between the peritectic and eutectic points of the liquidus line. Deviating from $SrPrGaO_4$, here is the additional possibility to grow the crystals in a range between the peritectic point and a certain concentration closer to the stoichiometric $ABCO_4$ composition.

4. Melt composition for crystal growth

Because of the incongruent melting behaviour of $SrPrGaO_4$ and $SrLaGaO_4$ the melt composition for the Czochralski growth must differ from that of the crystal. Generally, it may range between the peritectic and eutectic points of the liquidus line. The optimum melt composition, which leads to the highest yield at good quality, is basically located near the peritectic point but with liquidus temperature slightly below the incongruent melting temperature.

4.1. $SrPrGaO_4$

The investigation of various melt compositions tested for single crystal growth revealed a small region in the ternary phase diagram $SrO-Pr_2O_3-Ga_2O_3$ which allows the Czochralski growth of $SrPrGaO_4$ crystals (Fig. 5). This region was limited by the $SrO:Ga_2O_3$ ratios 1.82:1 and 1.67:1 and Pr_2O_3 contents between 24 and 28 mol%. Crystals with the best quality at a satisfactory yield were obtained from the starting melt composition of 48.1 mol% SrO, 25.65 mol% Pr_2O_3 and 26.25 mol% Ga_2O_3, i.e. this composition must be close to the peritectic point. The composition of $SrPrGaO_4$ single crystal grown from this melt, determined by the complexometric titration analysis and polarographic investigations was 53.4($\mp$0.7) mol% SrO, 23.5($\mp$0.3) mol% Pr_2O_3 and 23.1($\mp$0.2) mol% Ga_2O_3, i.e. the resulting chemical formula of the crystal is $Sr_{1.15}Pr_{1.02}Ga_{1.00}O_{4.18}$. That means, the composition shift from melt to crystal basically consists in the increase in the SrO content.

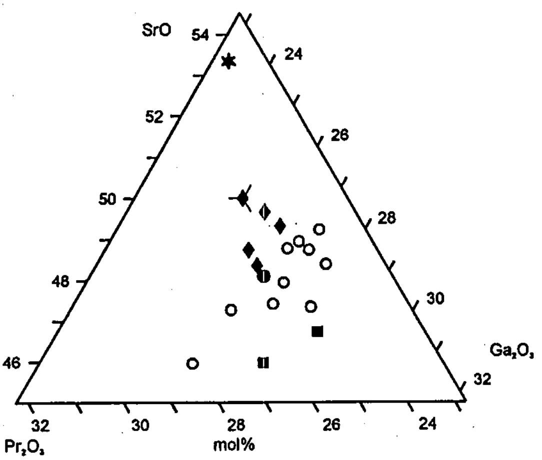

Fig. 5. Part of the ternary phase diagram $SrO-Pr_2O_3-Ga_2O_3$, o — single crystal growth, • — the best composition [mol%]: 48.1 SrO+25.65 Pr_2O_3+26.25 Ga_2O_3, full ◇ — primary crystallization of Sr_2PrGaO_5 above the peritectic decomposition temperature, ■ — crystallization of eutectic of $SrPrGa_3O_7$, $Pr_4Ga_2O_9$ and $SrPrGaO_4$, * — crystal composition.

If the SrO contents in the melt were risen above 48.2 mol% with nearly equal Pr_2O_3 and Ga_2O_3 concentrations, the peritectic point was exceeded and consequently, the Sr-rich phase Sr_2PrGaO_5 crystallized primarily, as detected by X-ray powder diffraction and energy dispersive X-ray spectroscopy (EDX) investigations.

When starting a Czochralski experiment from melts with SrO contents below about 46 mol% with like Pr_2O_3 and Ga_2O_3 concentrations, we obtained a polyphase product containing, as proved by the above techniques, $SrPrGaO_4$, $SrPrGa_3O_7$ and $Pr_4Ga_2O_9$, i.e. the components of the eutectic.

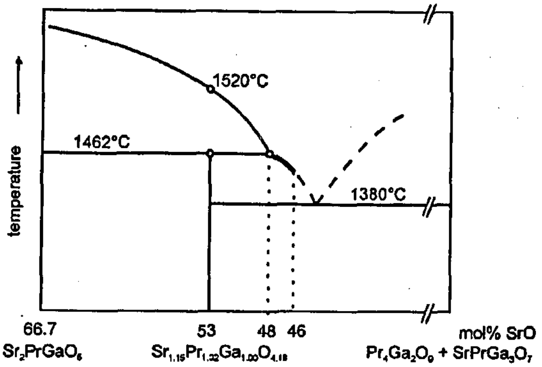

Fig. 6. Resulting pseudo-binary section of the phase diagram for $SrPrGaO_4$ crystallization.

The occurrence of the higher melting peritectic decomposition product Sr_2PrGaO_5, the determined crystal composition, the optimum melt composition and detection of the other constituents of the eutectic, $SrPrGa_3O_7$ and $Pr_4Ga_2O_9$, suggest the course of the crystallization of $SrPrGaO_4$ at/near the section SrO–$PrGaO_3$ of the ternary phase diagram (see Fig. 6).

4.2. SrLaGaO$_4$

Valuable investigations of the composition of the starting melt for $SrLaGaO_4$ were published by Dąbkowski et al. [4] in 1993. We have grown good crystals in the recommended area of the ternary phase diagram. Additionally, we found an extension of this area of appropriate melt compositions for $SrLaGaO_4$ growth, so that it nearly coincides with the melt compositions suitable for $SrPrGaO_4$. Nevertheless, crystals of the best optical homogeneity, at an acceptable yield, were grown from a melt composition published by Berkowski et al. [5]: 47.95 mol% SrO, 25.25 mol% La_2O_3, 26.80 mol% Ga_2O_3 (Fig. 7). Since Nakamura [6] has localized the peritectic point near 45 mol% SrO at equal La_2O_3 and Ga_2O_3 concentrations, the recommended melt composition is situated between the peritectic and the crystal composition, i.e. in the area of metastable crystallization.

The investigation of the $SrLaGaO_4$ crystal composition is under progress. Preliminary EDX and RFA investigations suggest compositions of about 53 mol% SrO, 24 mol% La_2O_3 and 23 mol% Ga_2O_3. Surely, the shift of the composition between melt and crystal is comparable to that observed for $SrPrGaO_4$, i.e. the crystal contains more strontium than the melt.

If the Sr contents of the melt are too high (more than 48.5 mol%), then only polycrystalline growth takes place, as observed by Dąbkowski et al. [4]. It is caused by primary crystallization of Sr_2LaGaO_5, as identified by X-ray powder diffraction and EDX.

Because we did not observe polyphase crystallization down to about 46 mol% SrO at nearly equal lanthanum and gallium oxide contents, the eutectic point will lie at lower strontium oxide contents as compared to $SrPrGaO_4$. Again, the eutectic

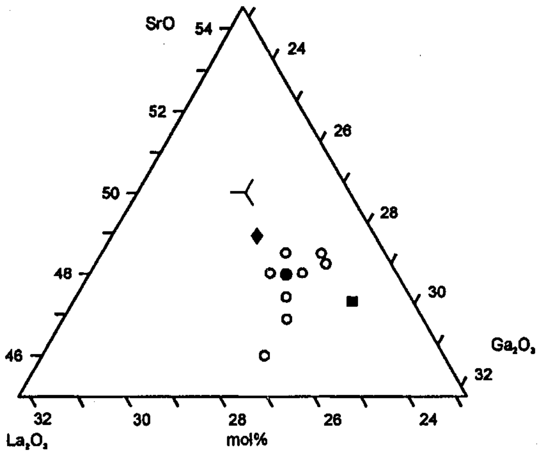

Fig. 7. Part of the ternary phase diagram SrO–La_2O_3–Ga_2O_3, o — single crystal growth, • — the best composition [mol%]: 47.95 SrO + 25.25 La_2O_3 + 26.80 Ga_2O_3, full ◇ — the primary crystallization of Sr_2LaGaO_5 above the peritectic decomposition temperature, ■ — crystallization of eutectic of $SrLaGa_3O_7$, $SrLa_2Ga_2O_7$ and $SrLaGaO_4$.

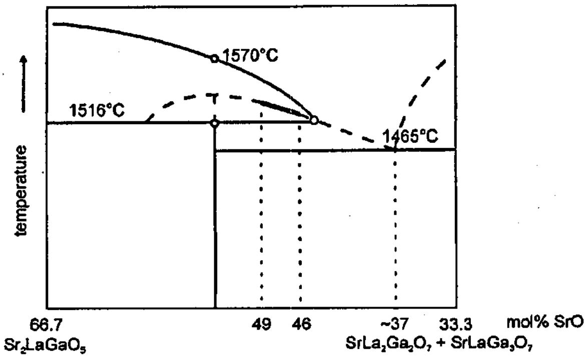

Fig. 8. Resulting pseudo-binary section of the phase diagram for $SrLaGaO_4$ crystallization.

phases were identified by the determination of the constituents of the residual melt after freezing. These are the following: $SrLaGaO_4$, $SrLaGa_3O_7$ and the so far unknown [6] phase $SrLa_2Ga_2O_7$. This last phase was identified by comparing its powder diffraction diagram with that of $SrNd_2Al_2O_7$ (PDF file 31-1334).

From the investigations of the accompanying phases of the growth process and the melt and crystal composition, we conclude that the course of crystallization of $SrLaGaO_4$ corresponds to that of the $SrPrGaO_4$, i.e. it proceeds at/near the section SrO–$LaGaO_3$ of the ternary phase diagram (see Fig. 8).

5. Yield

When growing crystals of an incongruently melting material by the Czochralski technique, the achievable yield of good quality single crystal materials depends mainly on width of the composition range between the peritectic and the eutectic points of the liquidus line. Consequently the starting melt composition for $SrPrGaO_4$ growth should be close to the upper limit of the allowed area shown in Fig. 5. In the special case of $SrLaGaO_4$, where crystallization is also possible above the incongruent melting temperature in a metastable equilibrium with the supercooled melt, the composition range of the starting melt can be extended beyond the peritectic point towards the crystal composition. This makes possible an unusual enlargement of the achievable yield.

Because the yield limitation by polyphase crystallization is a more severe problem in $SrPrGaO_4$ than in $SrLaGaO_4$, we will consider only $SrPrGaO_4$.

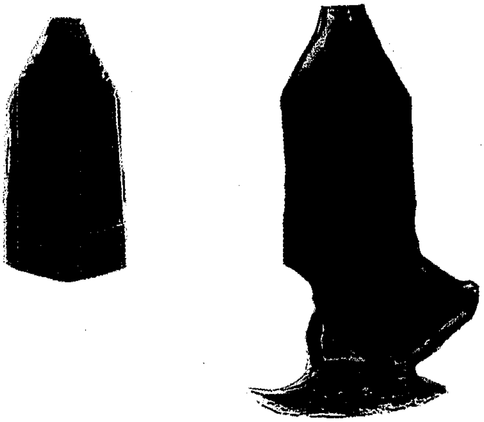

Fig. 9. $SrPrGaO_4$ crystals grown from the same melt, left: the growth finished before instabilities occur, right: the growth continued too long, leading to instabilities.

To determine the yields, we have measured the mass of crystals formed before polyphase crystallization begins. After exceeding this mass the growth instabilities occur. Figure 9 shows two crystals grown from the same melt compositions. Whereas the left crystal fully grew from a proper melt composition, the further prolongation of the right one led to a shift of the melt composition too close to the eutectic. This initiated local growth instabilities leading to spiral growth.

We have estimated the yields of four crystals grown from the proper melts exploiting between 34 and 39 mass% of the melt. For the residual melts one can estimate a Sr content of about 45 mol%. Probably this composition is not far from the eutectic, however one has to consider the effect of constitutional supercooling.

6. Constitutional supercooling

Constitutional supercooling principally cannot be avoided in incongruently melting systems. Generally it results in a deterioration of the crystal quality. Corresponding to the Tiller-criterion the onset of constitutional supercooling can be retarded by the selection of a proper melt composition and/or by appropriately adjusting growth rate and thermal conditions at the interface. The latter strongly influences the exchange of material in the melt just in front of the interface. This exchange is eventually affected by the macroscopic roughness of the interface. Because of the good exchange of material at the facets here the constitutional supercooling will be hampered. In contrast, in the cavities of the fractured non-faceted area of the interface the material exchange with the bulk melt is reduced. Subsequently the shift of the melt composition towards the eutectic composition will be locally accelerated and constitutional supercooling will be initiated preferentially

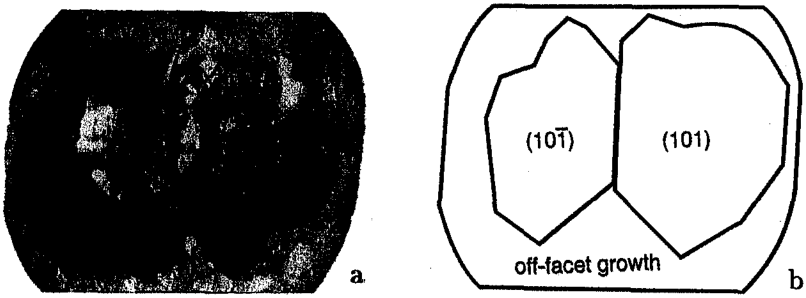

Fig. 10. Structure of the crystal-melt interface of a [100] $SrLaGaO_4$ crystal, (a) photo, (b) scheme of facets.

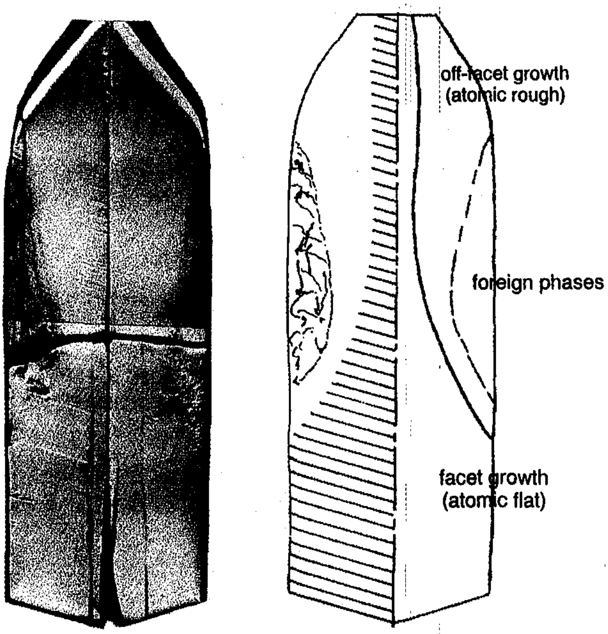

Fig. 11. Multiphase crystallization in the off-faceted region of a $SrLaGaO_4$ crystal.

here. Therefore, in $SrPrGaO_4$ and in $SrLaGaO_4$ growth one has to look for a fully faceted interface by adjusting the thermal gradients. This was achieved mainly by the proper choice of the active afterheater system.

Figure 10 shows the crystal-melt interface of a $SrLaGaO_4$ crystal. One can clearly distinct between flat facets and rough areas. Figure 11 demonstrates that only in the off-faceted area (rough) crystallization of a foreign phase took place. Differential thermoanalytical investigations of samples selected from the off-faceted grown regions revealed the occurrence of the eutectic.

7. Properties

7.1. Lattice constants

Lattice constants of the $SrPrGaO_4$ single crystals were determined using a four circle diffractometer CAD 4 (Mo K_α radiation): $a = 0.3813(2)$ nm, $c = 1.2532(6)$ nm. The $SrLaGaO_4$ lattice constants $a = 0.3843$ nm, $c = 1.268$ nm [7, 8] were confirmed.

However, we have observed in both crystals a set of weaker peaks, suggesting the occurrence of super structures. Their lattice constants are exactly twice those of the basic lattice. The influence of this super structure on the film deposition of YBCO still has to be investigated.

7.2. Colour of the $SrPrGaO_4$ crystals

The reported red stripes in the green $SrPrGaO_4$ single crystal were caused by Pr^{4+} ions as suggested by thermoanalytical investigations. DTA in air displayed complex endothermal melting effects, proving that redox equilibria can play an important role during melting and crystallization. Simultaneous TG-DTA measurements in different atmospheres gave some indications on the nature of the coloration:

- in air, freezing of the melt was accompanied by a mass decrease, reversible upon remelting; the frozen melt was coloured red to brown.
- in argon, no mass change was observed upon cooling or heating, the solidified melt was green.

These results suggest that the differences in colour are caused by a shift in the equilibrium of $Pr^{3+} \leftrightarrow Pr^{4+}$ during the crystallization. In air atmosphere the melt contains more Pr^{4+} than the solid, suggesting that Pr^{3+} is stabilized in the crystal lattice. From the mass change we can estimate that some 3–5% of the praseodymium ions were oxidized to Pr^{4+} upon melting in air atmosphere. Upon freezing, the majority of Pr^{4+} is again reduced to Pr^{3+}, but there remains some Pr^{4+} in the solid. Probably the red stripes contain an eutectic of $SrPrGaO_4$ and a strontium praseodymate (IV).

8. Summary

Both the most commonly used $ABCO_4$ substrate $SrLaGaO_4$, and the new $SrPrGaO_4$ crystal, show a troublesome behaviour during the Czochralski growth. These problems are due to the incongruent melting of the materials. Therefore, stoichiometric melt compositions cannot be used and proper melt compositions for single crystal growth had to be found. A principal way is suggested which allowed the identification of the SrO–(RE)GaO_3 section as that region of the ternary phase diagram SrO–$(RE)_2O_3$–Ga_2O_3, where the crystal growth proceeds. $SrLaGaO_4$ (but not $SrPrGaO_4$) can be grown starting from a metastable supercooled melt of a composition beyond the peritectic. For both materials, the unavoidable constitutional supercooling can be retarded by special growth conditions and by selecting the best melt composition. Both materials have lattice constants featuring a small mismatch to YBCO. The influence of the detected super structure on the film deposition still has to be investigated. The red coloured stripes of the $SrPrGaO_4$ crystals are caused by the presence of Pr^{4+} ions. Post-growth annealing in N_2+H_2 atmosphere reduces these Pr^{4+} ions and leads to homogeneously green crystals.

Acknowledgments

We thank U. Geißler and P.-M. Wilde for EDX investigations. Many thanks to M. Bernhagen for technical assistance.

References

[1] B.H.T. Chai, M. Long, in: *Proc. 2nd Eastern Regional Conf. on Crystal Growth, AACG/East 2, Atlantic City (NJ), October 1988*, AACG, Atlantic City 1988.

[2] M. Sasaura, S. Miyazawa, *J. Cryst. Growth* **166**, 825 (1996).

[3] P. Reiche, B. Hermoneit, D. Schultze, *Cryst. Res. Technol.* **20**, 845 (1985).

[4] A. Dąbkowski, H.A. Dąbkowska, J.E. Greedan, *J. Cryst. Growth* **132**, 205 (1993).

[5] M. Berkowski, A. Gloubokov, private communication.

[6] K. Nakamura, R. Katuno, I. Aoyama, *Phase Transit.* **42**, 99 (1993).

[7] JCPDS Powder Diffraction File 24-1208, 1974.

[8] S. Hontsu, J. Ishii, T. Kawai, S. Kawai, *Appl. Phys. Lett.* **59**, 2886 (1991).